24th COBEM - 2017

24th ABCM International Congress of Mechanical Engineering
December 3-8, 2017, Curitiba, PR, Brazil

COBEM-2017-1010
ON THE WHIRLING DIRECTION OF A PROBABILISTIC, UNDAMPED AND ASYMMETRIC LAVAL ROTOR MODEL SUBJECTED TO RESIDUAL UNBALANCE

Andreyson Bicudo Jambersi
Samuel da Silva
João Antonio Pereira
Antonio Eduardo Turra
[1]UNESP - Universidade Estadual Paulista "Júlio de Mesquita Filho", Faculdade de Engenharia de Ilha Solteira, Departamento de Engenharia Mecânica, Av. Brasil, 56, Centro, 15385-000, Ilha Solteira, SP, Brasil.
andreyson@dem.feis.unesp.br, samuel@dem.feis.unesp.br, japereira@dem.feis.unesp.br, turra@dem.feis.unesp.br

Abstract. *The main goal of this paper is to present a rotor modeled as an asymmetric and undamped Laval model subjected to residual unbalance which has uncertainties in the stiffness of its bearings, by using this model the backward whirling condition is identified. The motion equations of the rotor were described by complex coordinates to give information about the whirling direction according to the range of the spin speed in the rotor. The parametric stochastic model used considers the bearings stiffness as random variables and a Monte Carlo method is used to propagate their uncertainties. As results, it is possible to obtain the critical spin speed values, also called natural frequencies, and to identify the backward and forward whirling range of speeds, e.g. by assuming the uncertainties and considering it as a random variable. Some concerns about backward whirling are discussed and since it causes stress cycles of traction-compression in the shaft, it should be avoided. The probabilistic model obtained here has shown more robustness than a deterministic model in the backward whirling region.*

Keywords: *Undamped stochastic Laval rotor model. Jeffcott Model. Complex coordinates. Uncertainties. Monte Carlo simulation.*

1. INTRODUCTION

Rotors are widely used in machines and mechanisms in the industry to transfer energy from one point to another, providing numerous advantages since they assure efficiency, durability, and soft adjustments (Muszynska, 2005). In general, rotors can achieve high angular velocities and many important aspects of their dynamic behavior can imply in large vibration, instabilities or fatigue. Even in a theoretically well-balanced rotor, there is some level of residual unbalance that can affect the dynamics of the rotative system (Genta, 2007; Lalanne and Ferraris, 1998), for example for asymmetric rotors without or with low values of damping, the residual unbalance can produce whirl motion in two directions. The whirling direction is tightly associated with the state of stresses that arise in the shaft. Hull (1961) established a relationship between the backward direction of whirling motion and the traction-compression stresses cycles per shaft revolution. This increase of stress cycle is related to fatigue problems.

The whirling analysis has been commonly treated in terms of complex coordinates using a deterministic approach in literature (Lee, 1993; Mesquita, 2004). Nevertheless, the rotating systems can be treated considering stochastic parameters as can be seen in the recent works of Medina *et al.* (2007), Wang *et al.* (2009), Peradotto *et al.* (2015) and Ritto *et al.* (2015). Thus, in this paper, the whirling direction analysis is performed in terms of the complex coordinates of the center of mass, by modeling the stiffness of the bearings as random variables for a probabilistic and undamped asymmetric Laval rotor. A stochastic Monte Carlo simulation is used as a solver to propagates the uncertainties. Often, this class of method is appropriate for cases where there is only a small number of random variables inserted at the model (Schuëller, 1997). The identification of the whirling direction is performed directly from the diagram, that shows the amplitude ratio between forward and backward motion direction components, varying as a function of the spin speed of the rotative machine.

This paper is organized in six sections. First, the model of an undamped and asymmetric Laval rotor subjected to residual unbalance is described and its motion equations are shown in Section 2. Then, a deterministic model in complex coordinates is presented in Section 3 and the changing in the whirling direction is discussed in terms of forward and backward components. The Section 4 describe the model with stochastic parameters assumptions and the obtaining of the uncertain model. Section 5 shows the convergence analysis and simulation performed and some final remarks are

summarized in Section 6.

2. THE UNDAMPED ASYMMETRIC LAVAL ROTOR

The Laval rotor, also known as Jeffcott rotor (Genta, 2007), is considered one of the simplest model that can be used to study rotating systems. The Laval rotor is represented at Figure 1. Although being an oversimplification of the real-world, the Laval rotor contains some major characteristics of more complex systems in their response to unbalance (Ehrich, 1999). The modeling consists of assuming the disk as a concentrated-mass point attached to a massless flexible shaft and constrained by a restoring force, induced by the shaft and bearings stiffness. The mathematical description of the Laval rotor considering shaft flexibility is referred as a modified Jeffcott rotor model (Vance *et al.*, 2010). If the equivalent stiffness on x and y directions are identical, the rotor is said axially symmetrical; else, the system is asymmetrical, i.e. anisotropic. Often, anisotropy origins are on the bearings, in a way that values of shaft stiffness are equal in both directions x and y. The isotropic stiffness shaft is K and the anisotropic bearings stiffness are K_x and K_y. Thus, the equivalent stiffness along x and y axes are given by:

$$k_x = \frac{2K_xK}{2K_x + K}, \qquad k_y = \frac{2K_yK}{2K_y + K} \tag{1}$$

where k_x and k_y are the equivalent stiffness components (note the low-case characters that distinguish those from the bearing stiffness).

In practical applications, a rotor presents some residual unbalance. Hence, the center of mass P of the disk is offset from the elastic axis or geometric center C of the shaft (which is coincident with the geometric center of the disk), by an eccentricity (a radial distance) ϵ, as can be seen in Fig. 2. It produces a static unbalance $m\epsilon$ that affect the behavior of the whole system itself.

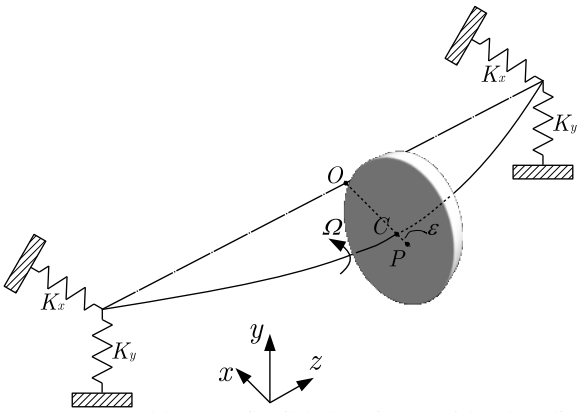

Figure 1. The undamped Laval rotor supported by two flexible bearings, with a bending shaft and a unbalance mass (the figure is intentionally out of proportions).

To explain this effect, a rigid shaft is considered at standstill position (e.g. with spin speed $\Omega = 0$). In this case, the points O and C are coincident, i.e., the shaft has no bending at all; likewise, in this condition the elastic and the rotation axes are coincident. Nonetheless, if the shaft is flexible, static flexural appears and the rotating axis moves from point O to C. Since spin speed increases, the centrifugal force of the eccentric mass makes point C to move outer and whirl about the rotation axis with a whirl radius $r_C(t)$, developing a radial distance between the rotating axis position and the elastic center of the shaft cross-section (Ehrich, 1999). Fig. 2 shows these coordinates represented in the x-y plane. Point P corresponds to the disk center of mass.

For a flexible shaft-bearings and undamped rotor subjected to a residual unbalance force and represented in the statically equilibrium position, the motion equations in Cartesian coordinates (Jeffcott, 1919) are given by:

$$m\ddot{x}_C + k_x x_C = m\epsilon\Omega^2 \sin(\Omega t) \tag{2}$$

$$m\ddot{y}_C + k_y y_C = m\epsilon\Omega^2 \cos(\Omega t) \tag{3}$$

where m is the mass of the rotor (considering a massless shaft), x_C and y_C are the position of the geometric center C of the shaft into both x and y axis direction, the second-order derivative terms $\ddot{x}_C$ and $\ddot{x}_C$ are the acceleration of C, ϵ is the eccentricity, Ω is the angular velocity. The detailed procedure to obtain these equations can be found in Lalanne and Ferraris (1998) and Genta (2007).

By these expressions, it is possible to observe that the system has two independent natural frequencies that do not depend on the spin speed of the rotor (Genta, 2007). Those frequencies are equal to the critical speeds, which are given

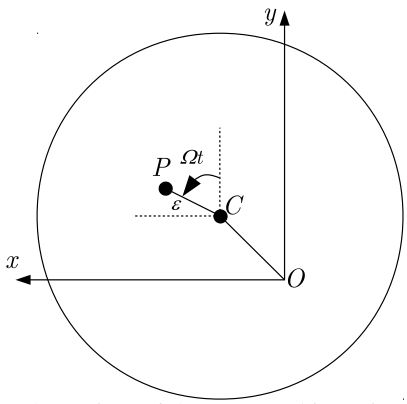

Figure 2. x-y plane view of the rotor and its points of interest.

by:

$$\Omega_{cr1} = \omega_{nx} = \sqrt{\frac{k_x}{m}}, \qquad \Omega_{cr2} = \omega_{ny} = \sqrt{\frac{k_y}{m}} \tag{4}$$

The Campbell diagram contains two horizontal straight lines (Genta, 2007), which is not true when damping is added in the model. As long as the free motions occur at different frequencies, the two harmonic motions cannot combine to generate circles or ellipses. In the first and second critical speeds, the motion reduces to a vibration along the x and y axis, respectively.

There is a direct relationship between the values of the spin speed band, with the natural frequencies of the rotor and the whirling of the unbalanced rotor. Lalanne and Ferraris (1998) identify those regimes of the whirl motion in terms of forward and backward motions accordingly to these values explicitly. Since the rotor is considered to be in well-aligned and the disk is in the center of the shaft, we do not take into account the gyroscopic effect or the gyroscopic whirling (the distinction between forward/backward modes of whirl and gyroscopic whirl is made by Lee (1993)).

3. THE LAVAL ROTOR IN COMPLEX COORDINATES: THE DETERMINISTIC MODEL

A complex coordinate $r_C(t)$ is defined by:

$$r_C(t) = y_C(t) + jx_C(t) \tag{5}$$

where $r_C(t)$ is the whirl radius (Lee, 1993), $y_C(t)$ and $x_C(t)$ are the components along the axis y and x, respectively and j is the imaginary unit.

Rewriting the motion equation in terms of $r(t)$:

$$m\underbrace{(\ddot{y}_C + j\ddot{x}_C)}_{=\ddot{r}_C} + k_y y_C + jk_x x_C = m\epsilon\Omega^2 \underbrace{(\cos(\Omega t) + j\sin(\Omega t))}_{=e^{j\Omega t}} \tag{6}$$

and, since the term $k_y y_C + jk_x x_C$ can be manipulated in the form:

$$k_y y_C + jk_x x_C = \left(\frac{k_y + k_y}{2}\right) y_C + j\left(\frac{k_x + k_x}{2}\right) x_C + \left(\frac{k_x - k_x}{2}\right) y_C + j\left(\frac{k_y - k_y}{2}\right) x_C \tag{7}$$

By introducing the mean stiffness k_m and the deviatoric stiffness k_d (Genta, 1999):

$$k_m = \left(\frac{k_x + k_y}{2}\right) \qquad \text{and} \qquad k_d = \left(\frac{k_y - k_x}{2}\right) \tag{8}$$

so, introducing these terms into eq. (7):

$$\begin{aligned} k_y y_C + jk_x x_C &= k_m y_C + k_d y_C + jk_m x_C - jk_d x_C \\ &= k_m \underbrace{(y_C + jx_C)}_{=r_C} + k_d \underbrace{(y_C - jx_C)}_{=\overline{r}_C} \\ &= k_m r_C + k_d \overline{r}_C \end{aligned} \tag{9}$$

where $\overline{r}_C$ is the conjugate of r_C. Then, the motion equation can be written as:

$$m\ddot{r}_C + k_m r_C + k_d \overline{r}_C = m\epsilon\Omega^2 e^{j\Omega t} \tag{10}$$

By assuming a proposed solution to the steady-state response due to unbalance forces:

$$r_C(t) = Q_f e^{j\Omega t} + Q_b e^{-j\Omega t} \tag{11}$$

$$\dot{r}_C(t) = j\Omega Q_f e^{j\Omega t} - j\Omega Q_b e^{-j\Omega t} \tag{12}$$

$$\ddot{r}_C(t) = -\Omega^2 Q_f e^{j\Omega t} + \Omega^2 Q_b e^{-j\Omega t} = -\Omega^2 \left(Q_f e^{j\Omega t} + Q_b e^{-j\Omega t}\right) \tag{13}$$

where the terms Q_f and Q_b are, respectively, the amplitudes of the forward and backward components of the response $r_C(t)$ and their values are dependent on the spin speed Ω. For simplification, this dependence will be omitted on the notation until the final expressions are obtained. So, $\overline{r}(t)$ is given by:

$$\overline{r}_C(t) = \overline{Q}_f e^{-j\Omega t} + \overline{Q}_b e^{j\Omega t} \tag{14}$$

By substituting equations (11), (13) and (14) into eq. (10):

$$-m\Omega^2 \left(Q_f e^{j\Omega t} + Q_b e^{-j\Omega t}\right) + k_m \left(Q_f e^{j\Omega t} + Q_b e^{-j\Omega t}\right) + k_d \left(\overline{Q}_f e^{-j\Omega t} + \overline{Q}_b e^{j\Omega t}\right) = m\epsilon\Omega^2 e^{j\Omega t} \tag{15}$$

by grouping the terms $e^{j\Omega t}$ and $e^{-j\Omega t}$:

$$e^{j\Omega t}\left[Q_f\left(-m\Omega^2 + k_m\right) + \overline{Q}_b k_d\right] = m\epsilon\Omega^2 e^{j\Omega t} \tag{16}$$

$$e^{-j\Omega t}\left[\overline{Q}_f k_d + Q_b\left(-m\Omega^2 + k_m\right)\right] = 0 \tag{17}$$

and applying the conjugate on eq. (17) and representing these equations in the matrix form, is possible to obtain the given non-trivial solution:

$$\begin{bmatrix} \left(-m\Omega^2 + k_m\right) & k_d \\ k_d & \left(-m\Omega^2 + k_m\right) \end{bmatrix} \begin{Bmatrix} Q_f \\ \overline{Q}_b \end{Bmatrix} = \begin{Bmatrix} m\epsilon\Omega^2 \\ 0 \end{Bmatrix} \tag{18}$$

as for the undamped case $\overline{Q}_b = Q_b$, this result can now be expressed in terms of Q_b:

$$\begin{bmatrix} \left(-m\Omega^2 + k_m\right) & k_d \\ k_d & \left(-m\Omega^2 + k_m\right) \end{bmatrix} \begin{Bmatrix} Q_f \\ Q_b \end{Bmatrix} = \begin{Bmatrix} m\epsilon\Omega^2 \\ 0 \end{Bmatrix} \tag{19}$$

After solving this system of equations by applying the Cramer's rule:

$$Q_f(\Omega) = \frac{m\epsilon\Omega^2\left(k_m - m\Omega^2\right)}{\left(k_m - m\Omega^2\right)^2 - k_d^2} \tag{20}$$

$$Q_b(\Omega) = \frac{-m\epsilon\Omega^2 k_d}{\left(k_m - m\Omega^2\right)^2 - k_d^2} \tag{21}$$

whereas $\omega_{nx} = \sqrt{\frac{k_x}{m}}$ and $\omega_{ny} = \sqrt{\frac{k_y}{m}}$, we have:

$$Q_f(\Omega) = \frac{\left(\omega_{nx}^2 + \omega_{ny}^2 - 2\Omega^2\right)\epsilon\Omega^2}{2\left(\Omega^2 - \omega_{nx}^2\right)\left(\Omega^2 - \omega_{ny}^2\right)} \tag{22}$$

$$Q_b(\Omega) = \frac{-\left(\omega_{nx}^2 - \omega_{ny}^2\right)\epsilon\Omega^2}{2\left(\Omega^2 - \omega_{nx}^2\right)\left(\Omega^2 - \omega_{ny}^2\right)} \tag{23}$$

The equations (22) and (23) are identical of the equation of the circle. Evidently, the response of the rotor is composed by the superposition of these two individual components, as functions of the spin speed Ω, and can generate circular or elliptical orbits. Considering $k_y > k_x$ as deterministic values, we can have five possible interesting scenarios:

1. When $|Q_f| \neq 0$ and $|Q_b| = 0$, case when $k_x = ky$ (symmetric rotor) the rotor has always circular orbit and forward whirl (synchronous with Ω);

2. When $|Q_f| = 0$ and $|Q_b| \neq 0$, the rotor has circular orbit and backward whirl (asynchronous with Ω);

3. When $\Omega < \omega_{nx} < \omega_{ny}$, then $\left|\frac{Q_f}{Q_b}\right| > |1|$ and the rotor has elliptical orbit with forward whirl;
4. When $\omega_{nx} < \Omega < \omega_{ny}$, then $\left|\frac{Q_f}{Q_b}\right| < |1|$ and the rotor has elliptical orbit with backward whirl. The unbalance mass has a phase angle of $180°$ in relation to the shaft;
5. When $\omega_{nx} < \omega_{ny} < \Omega$, then $\left|\frac{Q_f}{Q_b}\right| > |1|$ and the rotor has elliptical orbit with forward whirl.

From the point of view of Strength of Materials, backward whirling can be a problem since a single-frequency backward whirl produces two stress cycles (traction-compression) per shaft revolution. This condition occurs in the fourth scenario, when the spin speed value is between the two critical speeds ($\omega_{nx} < \Omega < \omega_{ny}$) (Lee, 1993).

In asymmetric rotors in cases when both shaft and bearings are anisotropic, another concerning case can exist, the double-frequency backward whirl, where there are three stress cycles per revolution (Hull, 1961). The increase of stress cycles causes the reduction of the life cycle of the shaft, propagating cracks and causing fatigue.

4. THE LAVAL ROTOR IN COMPLEX COORDINATES: THE STOCHASTIC MODEL

For the deterministic case, where the rotor parameters have well-known predefined value and perform the identification of the operating regime of the rotor can be a quite simple scenario, those values are determined by well-delimited single lines. There are some interesting papers that describe those results in the literature, as for instance Lee (1993), Lalanne and Ferraris (1998), Mesquita (2004) and Genta (2007).

On the other side, in cases where there are uncertainties in some parameters of the rotor, those transition zones between forward/backward whirl motion cannot be defined as a single number/line anymore, but, rather, as a range of values. The same can be said about the natural frequencies, that will be no longer a value unique anymore.

Here the probabilistic approach is used and consists into randomize the bearings stiffness, due to the system high sensibility expected for its variation, and adopt a simple stochastic model for these variables, assuming them to be independent with well-known distributions. Thus, the data uncertainties are assumed as well represented in a probabilistic environment. This approach uses probability theory to model uncertainties as random mathematical objects (Cunha Jr, 2017).

In order to obtain a stochastic model, some random variables must be introduced into it. The probability space (Θ,$\mathcal{A}$,$\mathbb{P}$) is defined, where Θ is the sample space, where each element of Θ is a combination of cause states affecting the state of the system (Krée, 1986). $\mathcal{A}$ is a σ-algebra (or Borel field) on Θ (i.e., the possible events) with a probability measure $\mathbb{P}$. It is assumed that any random variable is a mapping $\mathbb{X} : \Theta \mapsto\in \mathbb{R}$, in which the preimage of every real number is a relevant event with probability distribution $P_{\mathbb{X}}(x)$ on $\mathbb{R}$ and admits a probability density function (PDF) $x \mapsto p_{\mathbb{X}}$, with respect to dx, i.e., the random variable is a function from the set of sample points to the set of real values (Gallager, 2012).

For the Laval rotor model described in the last section, the bearings stiffness K_x and K_y are assumed to be uncertain. Thereby, the equivalent, mean and deviatoric stiffness, k_x, k_y, k_m and k_d, as long as the natural frequencies ω_{nx} and ω_{ny} and the components Q_f and Q_b of the response, must be assumed as uncertain as well, since their values depends on K_x and K_y. So, modeling those values as random variables, we have, $\theta \in \Theta \mapsto \mathbb{K}_x(\theta)$, $\mathbb{K}_y(\theta)$, $\Bbbk_x(\theta)$, $\Bbbk_y(\theta)$, $\Bbbk_m(\theta)$, $\Bbbk_d(\theta)$, $\mathfrak{w}_{nx}(\theta)$, $\mathfrak{w}_{ny}(\theta)$, $\mathbb{Q}_f(\theta,\Omega)$, $\mathbb{Q}_b(\theta,\Omega)$. Hereby, the stochastic equivalent of equations (22) and (23) are given by:

$$\mathbb{Q}_f(\Omega) = \frac{\left(\mathfrak{w}_{nx}^2 + \mathfrak{w}_{ny}^2 - 2\Omega^2\right)\epsilon\Omega^2}{2\left(\Omega^2 - \mathfrak{w}_{nx}^2\right)\left(\Omega^2 - \mathfrak{w}_{ny}^2\right)} \tag{24}$$

$$\mathbb{Q}_b(\Omega) = \frac{-\left(\mathfrak{w}_{nx}^2 - \mathfrak{w}_{ny}^2\right)\epsilon\Omega^2}{2\left(\Omega^2 - \mathfrak{w}_{nx}^2\right)\left(\Omega^2 - \mathfrak{w}_{ny}^2\right)} \tag{25}$$

where the random processes $(\theta,t) \in \Theta \times \mathbb{R} \mapsto \mathbb{Q}_f(\theta,t)$, $(\theta,t) \in \Theta \times \mathbb{R} \mapsto \mathbb{Q}_b(\theta,t)$ are the forward and backward components of the response. This formulation is based on the hypothesis that the terms $\mathbb{K}_x$ and $\mathbb{K}_y$ are independent random variables.

5. PARAMETERS OF THE ROTOR AND THE NUMERICAL SIMULATION RESULTS

As mentioned earlier, the assumed stochastic Laval model considers the stiffness parameters as random variables. As a consequence, the response of the system will no longer be a number anymore, but also a random variable, that is, the expected value of the output random variable (Aguirre, 2015). The stiffness of the bearings was assumed as stochastic variables with a Γ distribution and a confidence band of 99% of probability. Probability density function of the Γ distribution is given by:

$$p_{\mathbb{X}}(x) = \frac{1}{\Gamma(k)\theta^k} x^{(k-1)} e^{(-x/\theta)} \mathbb{1}_{(0,+\infty)}(x) \tag{26}$$

A Monte Carlo numerical method is used to solve the equations by performing the propagation of uncertainties. An overview of stochastic modeling of uncertainties applied in structural dynamics can be found in Soize (2013), while most general applications and the background of the Monte Carlo method are discussed in Kroese *et al.* (2013).

The mean values and the coefficients of variation of the stiffness of the bearings $\mathbb{K}_x$ and $\mathbb{K}_y$, as well as the deterministic parameters of the rotor, are presented on Tab. 1 and were chosen based on Idehara (2003). The probabilistic density function of the stiffness of the bearings was assumed as a γ distribution as suggested by Soize (2017). The variables $\mu_{\mathbb{K}_x}$ and $\mu_{\mathbb{K}_y}$ are the mean values of $\mathbb{K}_x$ and $\mathbb{K}_y$ and also, $\delta_{\mathbb{K}_x}$ and $\delta_{\mathbb{K}_y}$ are their coefficient of variation.

Table 1. Parameters of the rotor used in the simulations.

Parameter	**Value** [unit]
m	1 [kg]
e	1×10^{-3} [m]
K	0.5×10^{3} [kN/m]
$\mu_{\mathbb{K}_x}$	0.2×10^{3} [kN/m]
$\mu_{\mathbb{K}_y}$	1.6×10^{3} [kN/m]
$\delta_{\mathbb{K}_x}$	0.05
$\delta_{\mathbb{K}_y}$	0.05

The uncertainties on the bearing stiffness can be related to several issues that are difficult to take into account, as its variation accordingly to angular position (Sunnersjö, 1978; While, 1979), linear assumption for the model (While, 1979), bearings stiffness value variations in function of a vast number of parameters, e.g., preload, clearance, several dismantling and reassembling, temperature, lubricant properties, and excitation force (Stone, 1982). Different methods can also be used to identify and to update the stiffness values often producing dissimilar results (Kraus *et al.*, 1987) and even in cases where the parameters are theoretically well calculated, inaccuracies can be expected due to the numerical method used or non-linear behavior (Medina *et al.*, 2008).

The simulation was performed using $N = 500$ sample points for each $\mathbb{K}_x$ and $\mathbb{K}_y$. This number of points gave $N_s = 500^2 = 250000$ Monte Carlo realizations for the equivalent stiffness values $\Bbbk_x$ and $\Bbbk_y$, for the natural frequencies $\mathfrak{w}_{nx}$ and ω_{ny}, for the complexes variables $\mathbb{Q}_f(\Omega)$ and $\mathbb{Q}_b(\Omega)$ calculation for each value of Ω.

Convergence analysis of the stochastic solution can be done using $\mathscr{L}_2$ norm of the difference between two successive approximations as a metric. The PDFs (probability density functions) of the stiffness $\mathbb{K}_x$ and $\mathbb{K}_y$ were generated from the histograms of the variables for the N_s number of points.

5.1 STOCHASTIC SOLUTION CONVERGENCE ANALYSIS

At first, it is analyzed the convergence of the Monte Carlo simulation for the parameters $\mathbb{Q}_f(\Omega)$, $\mathbb{Q}_b(\Omega)$ and $\left|\frac{\mathbb{Q}_f}{\mathbb{Q}_b}\right|(\Omega)$. This analysis is necessary in order to evaluate the convergence of the Monte Carlo simulation to a number of N_s realization and can be done according to Eq. (27) (Soize, 2005). The Galerkin method is used, and it takes in consideration the $\mathscr{L}_2$ norm of the difference between two successive approximations as a metric (Cunha Jr and Sampaio, 2014). The convergence is defined as:

$$conv(n_s) = \left\{ \frac{1}{n_s} \sum_{k=1}^{n_s} \int_{\Omega \in \mathcal{B}} \left\| \mathbf{Q}^n \left(\Omega; \theta_k \right) \right\|^2 d\Omega \right\}^{1/2} \tag{27}$$

Figure 3 shows the convergence of $\mathbb{Q}_f$ and $\mathbb{Q}_b$ for $N_s = 500^2 = 250000$ points. It is possible to notice that both converges quickly. The convergence of the stochastic solution for $\left|\frac{\mathbb{Q}_f}{\mathbb{Q}_b}\right|$ was also analyzed in terms of the mean-square, as presented on eq. (27) and it is shown on Fig. 4. Hence, is possible to notice that steady state is cleared reached for $n_s > 1.2 \times 10^5$ points and the results obtained for $\left|\frac{\mathbb{Q}_f}{\mathbb{Q}_b}\right|$ as a function of Ω is reliable.

Figure 5 shows the PDF's of the stochastic variables $\mathbb{K}_x$ and $\mathbb{K}_y$.

Figure 6 shows $\left|\frac{\mathbb{Q}_f}{\mathbb{Q}_b}\right|$ as a function of the spin speed Ω. Here, the vertical solid lines represent the critical speeds, in rpm. It is possible to observe that, instead having only one value, now there is a range of values limited by the dotted red lines. The mean values of $\left|\frac{\mathbb{Q}_f}{\mathbb{Q}_b}\right|$ for each value of Ω are given by the blue line inside the gray envelope, that is the confidence band of 99% of probability.

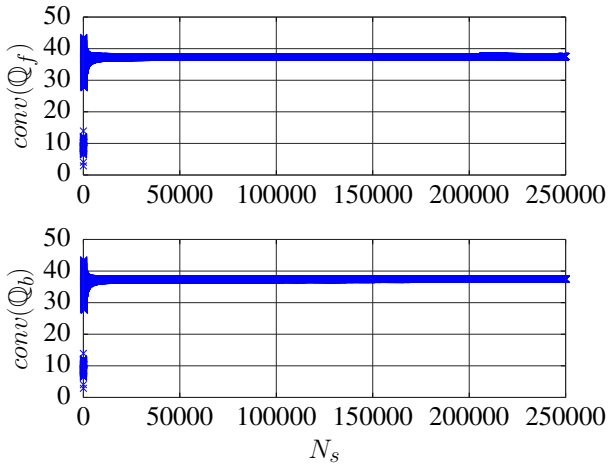

Figure 3. Convergence of $\mathbb{Q}_f$ and $\mathbb{Q}_b$ individually, using $N_s = 250000$ Monte Carlo realizations.

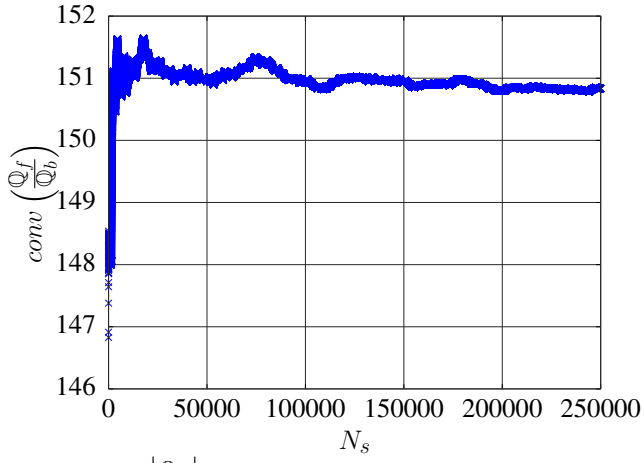

Figure 4. PDF of $\left|\frac{\mathbb{Q}_f}{\mathbb{Q}_b}\right|$ using $N_s = 250000$ Monte Carlo realizations.

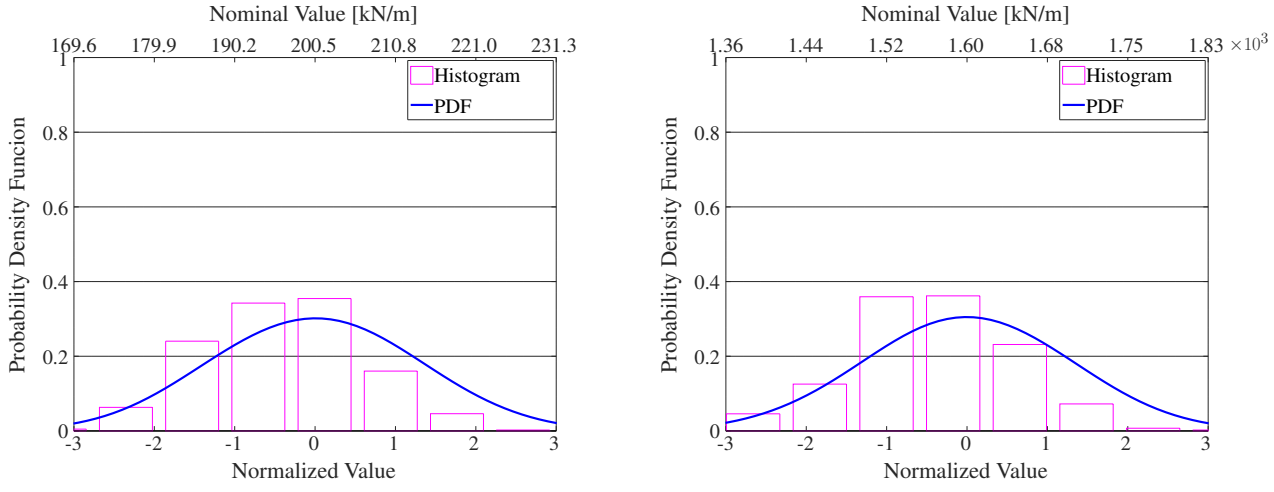

(a) Histogram and PDF of $\mathbb{K}_x$.

(b) Histogram and PDF of $\mathbb{K}_y$.

Figure 5. Histograms and PDFs of $\mathbb{K}_x$ and $\mathbb{K}_y$, using $N_s = 250000$ Monte Carlo realizations.

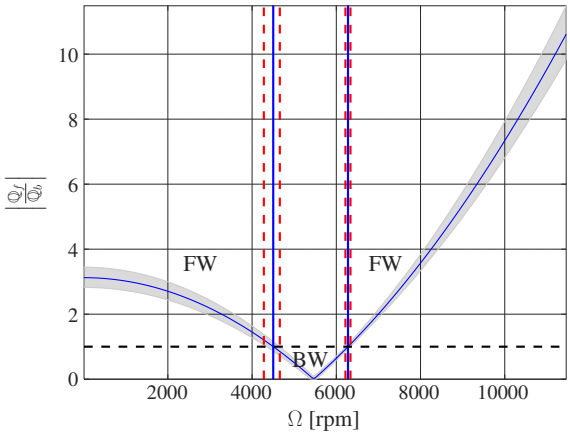

Figure 6. $\left|\frac{\mathbb{Q}_f}{\mathbb{Q}_b}\right|(\Omega)$ as a function of Ω for $N_s = 250000$ Monte Carlo realizations.

Figure 7 shows the PDF's of the natural frequencies ω_{nx} and ω_{ny}. The first critical speed ω_{nx} has a larger envelope than the second one. So, in cases when $\left|\frac{\mathbb{Q}_f}{\mathbb{Q}_b}\right| < 1$ for the forward-to-backward whirling direction determination, it should be taken it into consideration.

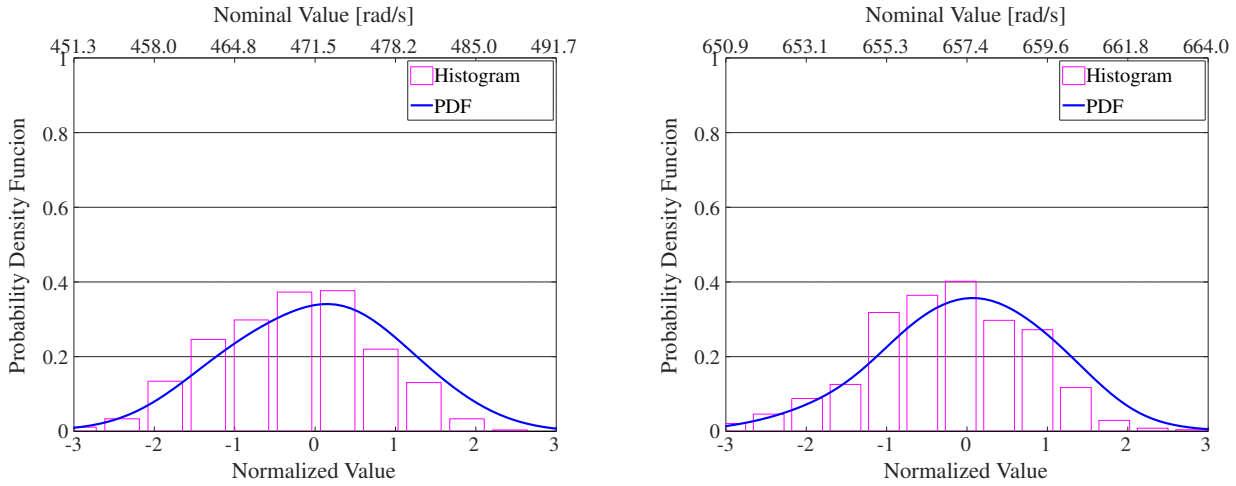

(a) Histogram and PDF of ω_{nx}.

(b) Histogram and PDF of ω_{ny}.

Figure 7. Histograms and PDFs of ω_{nx} and ω_{ny}, using $N_s = 250000$ Monte Carlo realizations.

Next steps of this work include the development and analysis of a damped asymmetric Laval model and experimental tests, to verify and calibrate the stochastic model suggested in the present work.

6. FINAL REMARKS

An undamped and asymmetric Laval model was proposed, in a way to verify some of the characteristics of a rotor subjected to its residual unbalance, taking into account some uncertainties in its stiffness parameters. An uncertain diagram obtained presents the forward and backward whirling direction in function of spin speed.

The deterministic model and its outputs vibration were already extensively treated by literature in several works previously and, in those cases, the whirling direction can be well-defined and easily identifiable. Indeed, by using the deterministic approach, the regions that boarded the forward and backward whirling are described in terms of simple lines with well-delimited boundaries. However, the identification of the whirling direction can be a challenge in cases where some of the parameters are uncertain. In those cases, instead of lines, there is a range of possible values where, a priori, is not possible to determine exactly the whirling direction and it is required a stochastic model. Here, the stiffness of the bearings was assumed as stochastic variables with Γ distribution. The response of the rotor was obtained using Monte Carlo simulations and was described in terms of complex coordinates, to give the forward and backward amplitudes by varying as functions of the spin speed.

An uncertain diagram was identified for $\left|\frac{\mathbb{Q}_f}{\mathbb{Q}_b}\right|(\Omega)$ in a way to obtain information about the whirling direction. This

diagram could be useful for preliminary decisions to predict which range of spin speed should be avoided. Additionally, a procedure can be proposed to identify the PDF of the stiffness based in the vibration outputs.

7. ACKNOWLEDGEMENTS

The first author would like to thank FEPISA (Fundação de Ensino, Pesquisa e Extensão de Ilha Solteira) and CAPES (Coordenação de Aperfeiçoamento de Pessoal de Nível Superior) for their doctoral scholarship. The authors also thank the financial support provided by CAPES, CNPq (Conselho Nacional de Desenvolvimento Científico e Tecnológico) and FEPISA.

8. REFERENCES

Aguirre, L.A., 2015. *Introdução à identificação de sistemas: Técnicas lineares e não lineares: teoria e aplicação*. Editora UFMG.

Cunha Jr, A., 2017. "Modeling and quantification of physical systems uncertainties in a probabilistic framework". In *Probabilistic Prognostics and Health Management of Energy Systems*, Springer, pp. 127–156.

Cunha Jr, A. and Sampaio, R., 2014. "Effects of a random cubic spring on the longitudinal dynamics of a bar excited by a gaussian white noise". In *2nd International Symposium on Uncertainty Quantification and Stochastic Modeling (Unceranties 2014), Rouen, France*.

Ehrich, F., 1999. *Handbook of Rotordynamics*. Krieger Publishing Company. ISBN 9781575240886. URL https://books.google.com.br/books?id=2L7iAAAAMAAJ.

Gallager, R.G., 2012. *Discrete stochastic processes*, Vol. 321. Springer Science & Business Media.

Genta, G., 1999. *Vibration of Structures and Machines: Practical Aspects*. Springer New York. ISBN 9780387985060. URL https://books.google.com.br/books?id=pxXNIluJXLgC.

Genta, G., 2007. *Dynamics of rotating systems*. Springer Science & Business Media.

Hull, E.H., 1961. "Shaft whirling as influenced by stiffness asymmetry". *Int. J. Non-linear Mech*, Vol. 83, pp. 219–226.

Idehara, S., 2003. *Aplicação de Técnicas de Order Tracking para a Análise de Máquinas e Componentes Rotativos*. Master's thesis, Universidade Estadual de Campinas.

Jeffcott, H.H., 1919. "XXVII. the lateral vibration of loaded shafts in the neighbourhood of a whirling speed: The effect of want of balance". *The London, Edinburgh, and Dublin Philosophical Magazine and Journal of Science*, Vol. 37, No. 219, pp. 304–314.

Kraus, J., Blech, J. and Braun, S., 1987. "In situ determination of rolling bearing stiffness and damping by modal analysis". *ASME, Transactions, Journal of Vibration, Acoustics, Stress, and Reliability in Design*, Vol. 109, pp. 235–240.

Krée, P.; Soize, C., 1986. *Mathematics of random phenomena: random vibrations of mechanical structures*, Vol. 32. D. Reidel Publishing Company.

Kroese, D.P., Taimre, T. and Botev, Z.I., 2013. *Handbook of monte carlo methods*, Vol. 706. John Wiley & Sons.

Lalanne, M. and Ferraris, G., 1998. *Rotordynamics prediction in engineering*. Number v. 2 in Rotordynamics prediction in engineering. John Wiley. ISBN 9780471972884. URL https://books.google.com.br/books?id=JONSAAAAMAAJ.

Lee, C., 1993. *Vibration Analysis of Rotors*. Solid Mechanics and Its Applications. Springer Netherlands. ISBN 9780792323006. URL https://books.google.com.br/books?id=ueK86Qjs42AC.

Medina, L., Ruiz, R. and Díaz, S., 2008. "A simple approach to determine uncertainty bounds on bearing rotordynamic coefficients identification". In *ASME Turbo Expo 2008: Power for Land, Sea, and Air*. American Society of Mechanical Engineers, pp. 1279–1287.

Medina, L., Ruiz, R., Díaz, S. and de Máquinas, L.d.D., 2007. "A simple approach to determine uncertainty bounds on bearing rotordynamic coefficients identification". *Artículo inédito, Universidad Simón Bolívar. Sartenejas, Edo Miranda. Venezuela*.

Mesquita, A.L.A., 2004. *Identificação de modos operacionais e naturais de vibração em maquinas rotativas utilizando coordenadas complexas*. Ph.D. thesis, Universidade Estadual de Campinas.

Muszynska, A., 2005. *Rotordynamics*. CRC press.

Peradotto, E., Salles, L., Panunzio, A. and Schwingshackl, C., 2015. "Stochastic methods for nonlinear rotordynamics with uncertainties". *Proceedings of the Turbo Expo*.

Ritto, T.G., Maldonado, D.J.G. and de Deus, P.A.L., 2015. "Robust campbell diagram of a simple 2dof rotordynamic system". In *23rd ABCM International Congress of Mechanical Engineering*.

Schuëller, G.I., 1997. "A state-of-the-art report on computational stochastic mechanics". *Probabilistic Engineering Mechanics*, Vol. 12, No. 4, pp. 197–321.

Soize, C., 2017. *Uncertainty Quantification: An Accelerated Course with Advanced Applications in Computational Engineering*. Interdisciplinary Applied Mathematics. Springer International Publishing. ISBN 9783319543390. URL https://books.google.com.br/books?id=nmy8DgAAQBAJ.

Soize, C., 2005. "A comprehensive overview of a non-parametric probabilistic approach of model uncertainties for predictive models in structural dynamics". *Journal of sound and vibration*, Vol. 288, No. 3, pp. 623–652.

Soize, C., 2013. "Stochastic modeling of uncertainties in computational structural dynamics-recent theoretical advances". *Journal of Sound and Vibration*, Vol. 332, No. 10, pp. 2379–2395.

Stone, B., 1982. "The state of the art in the measurement of the stiffness and damping of rolling element bearings". *CIRP Annals-Manufacturing Technology*, Vol. 31, No. 2, pp. 529–538.

Sunnersjö, C., 1978. "Varying compliance vibrations of rolling bearings". *Journal of sound and vibration*, Vol. 58, No. 3, pp. 363–373.

Vance, J.M., Zeidan, F.Y. and Murphy, B., 2010. *Machinery vibration and rotordynamics*. John Wiley & Sons.

Wang, Q., Pettinato, B. and Maslen, E., 2009. "Identification in rotordynamics: uncertainty analysis and quality estimation". *ASME Paper No. GT2009-59103*.

While, M., 1979. "Rolling element bearing vibration transfer characteristics: effect of stiffness". *ASME J. Appl. Mech*, Vol. 46, pp. 677–684.

9. RESPONSIBILITY NOTICE

The authors are the only responsible for the printed material included in this paper.